ANATOMICAL PATHOLOGY

Aberrant protein expression of Appl1, Sortilin and Syndecan-1 during the biological progression of prostate cancer

Carmela Martini[1,*], Jessica M. Logan[1,*], Alexandra Sorvina[1,*], Colin Gordon[1], Andrew R. Beck[1], Ben S-Y. Ung[1], Maria C. Caruso[1], Courtney Moore[1], Ashleigh Hocking[2], Ian R. D. Johnson[1], Ka Lok Li[1], Litsa Karageorgos[1], Ashley M. Hopkins[4], Adrian J. Esterman[1], Chelsea Huzzell[1], Robert D. Brooks[1], Joanna Lazniewska[1], Shane M. Hickey[1], Christie Bader[1], Emma Parkinson-Lawrence[1], Roberto Weigert[3], Michael J. Sorich[4], Prerna Tewari[5], Cara Martin[5], Sharon O'Toole[5], Mark Bates[5], Mark Ward[5], Bashir Mohammed[5], Helen Keegan[5], William Watson[6], Sophie Prendergast[7], Sheena Heffernan[7], Sarah NiMhaolcatha[7], Roisin O'Connor[7], Victoria Malone[7], Marguerite Carter[7], Katie Ryan[7], Nathan Brady[7], Andres Clarke[7], Filip Sokol[7], Sarita Prabhakaran[1,2], Jürgen Stahl[8], Sonja Klebe[2,9], Hemamali Samaratunga[10], Brett Delahunt[11], Stavros Selemidis[12], Kim L. Moretti[13,14,15], Lisa M. Butler[16,17], John J. O'Leary[5,†], Douglas A. Brooks[1]

[1]Clinical and Health Sciences, University of South Australia, Adelaide, SA, Australia; [2]Department of Anatomical Pathology, College of Medicine and Public Health, Flinders University, Adelaide, SA, Australia; [3]Center for Cancer Research, National Cancer Institute, Bethesda, MD, USA; [4]College of Medicine and Public Health, Flinders University, Flinders Drive, Bedford Park, Adelaide, SA, Australia; [5]Department of Histopathology, Trinity College Dublin, Dublin, Ireland; [6]University College Dublin, School of Medicine, Conway Institute, University College Dublin, Dublin, Ireland; [7]Department of Pathology, The Coombe Women and Infants University Hospital, Dublin, Ireland; [8]Department of Cytopathology and Histopathology, Clinpath Pathology, Adelaide, SA, Australia; [9]Department of Surgical Pathology, SA Pathology at Flinders Medical Centre, Adelaide, SA, Australia; [10]Aquesta Uropathology and the University of Queensland, Brisbane, Qld, Australia; [11]Department of Pathology and Molecular Medicine, Wellington School of Medicine and Health Sciences, University of Otago, Wellington, New Zealand; [12]School of Health and Biomedical Sciences, STEM College, RMIT University, Bundoora, Melbourne, Vic, Australia; [13]Discipline of Surgery, University of Adelaide, Adelaide, SA, Australia; [14]University of South Australia, Adelaide, SA, Australia; [15]Faculty of Medicine, Nursing and Health Sciences, Monash University, Melbourne, Vic, Australia; [16]South Australian ImmunoGENomics Cancer Institute and Freemasons Centre for Male Health and Wellbeing, University of Adelaide, Adelaide, SA, Australia; [17]Solid Tumour Program, Precision Cancer Medicine Theme, South Australian Health and Medical Research Institute, Adelaide, SA, Australia; *co-first authors. †co-senior authors.

Summary

Diagnosis and assessment of patients with prostate cancer is dependent on accurate interpretation and grading of histopathology. However, morphology does not necessarily reflect the complex biological changes occurring in prostate cancer disease progression, and current biomarkers have demonstrated limited clinical utility in patient assessment. This study aimed to develop biomarkers that accurately define prostate cancer biology by distinguishing specific pathological features that enable reliable interpretation of pathology for accurate Gleason grading of patients. Online gene expression databases were interrogated and a pathogenic pathway for prostate cancer was identified. The protein expression of key genes in the pathway, including adaptor protein containing a pleckstrin homology (PH) domain, phosphotyrosine-binding (PTB) domain, and leucine zipper motif 1 (Appl1), Sortilin and Syndecan-1, was examined by immunohistochemistry (IHC) in a pilot study of 29 patients with prostate cancer, using monoclonal antibodies designed against unique epitopes. Appl1, Sortilin, and

Syndecan-1 expression was first assessed in a tissue microarray cohort of 112 patient samples, demonstrating that the monoclonal antibodies clearly illustrate gland morphologies. To determine the impact of a novel IHC-assisted interpretation (the utility of Appl1, Sortilin, and Syndecan-1 labelling as a panel) of Gleason grading, versus standard haematoxylin and eosin (H&E) Gleason grade assignment, a radical prostatectomy sample cohort comprising 114 patients was assessed. In comparison to H&E, the utility of the biomarker panel reduced subjectivity in interpretation of prostate cancer tissue morphology and improved the reliability of pathology assessment, resulting in Gleason grade redistribution for 41% of patient samples. Importantly, for equivocal IHC-assisted labelling and H&E staining results, the cancer morphology interpretation could be more accurately applied upon re-review of the H&E tissue sections. This study addresses a key issue in the field of prostate cancer pathology by presenting a novel combination of three biomarkers and has the potential to transform clinical pathology practice by standardising the interpretation of the tissue morphology.

INTRODUCTION

Confirming the diagnosis for a patient with prostate cancer and assessing the prognosis is reliant on an accurate interpretation of histopathology. Prostate cancer tissue morphology is assessed on routine haematoxylin and eosin (H&E) stained sections, using established diagnostic criteria for malignancy, and is Gleason graded according to modifications of the system developed by Gleason in 1966.[1] This grading system has undergone many iterations in an attempt to correlate the results more accurately with outcome and enable more reliable prognostication.[2–6] Despite these changes, the subjectivity of morphological assessment remains an issue for pathologists.[7–10]

Gleason defined five grades relating to prognosis, but the boundaries between these can be confounding. In particular, the differentiation between well formed and poorly formed glands, tangential cutting artifacts, and distinguishing benign mimics of malignancy from cancer are recognised problems.[11,12] While there are no gold standard prostate cancer biomarkers that address these issues, immunohistochemical (IHC) labelling has been widely utilised to aid morphological assessment. For example, α-methylacyl-CoA racemase (AMACR), a soluble peroxisomal and mitochondrial enzyme that is variably expressed in prostate cancer, in combination with basal cell markers (P63, 34βE12 and cytokeratin 5/6), can be employed to differentiate benign from malignant glands. However, this cocktail has limited clinical utility for grading as it does not distinguish between benign mimics or between different prostate cancer morphologies.[13–16] New biomarkers are required to identify critical cancer pathogenesis to improve the reliability of morphological assessment,

as effective prognosis, management and treatment of patients with prostate cancer heavily relies on accurate grading.

Previous investigations have shown that endosome-lysosome biogenesis is significantly and consistently altered in prostate cancer compared to non-malignant cells and tissue.[17–19] Indeed, the endosome-lysosome system has direct functional links to all major hallmarks of cancer pathology.[20–22] For example, endosomes and lysosomes control vesicular traffic, intracellular communication, immune function/inflammation, cellular uptake of nutrients, macromolecular degradation, energy metabolism and sensing, cytokinesis, cytokine signalling, interactions with the microenvironment and cell division (see recent review).[23] This current study aimed to investigate the expression of three endosomal biomarkers, adaptor protein containing a pleckstrin homology (PH) domain, phosphotyrosine-binding (PTB) domain, and leucine zipper motif 1 (Appl1), Sortilin, and Syndecan-1, in the progression of prostate cancer. Furthermore, the study addressed the impact of a novel biomarker IHC-assisted analysis on the reliability of Gleason grading. It was postulated that alterations in the expression of specific endosome-lysosome proteins can accurately define prostate cancer pathogenesis, which may have important implications for the clinical management of patients.

MATERIALS AND METHODS

Patient information

The retrospective pilot cohort comprised transurethral resection of the prostate (TURP) samples from 29 patients obtained through the Australian Prostate Cancer Bioresource (APCB), according to their recruitment criteria. A larger test cohort of 112 patients from a previously constructed Tissue Microarray (TMA) was accessed from Flinders Medical Centre (FMC; Supplementary Table 1, Appendix A), Adelaide, Australia.[24] The expansion cohort comprised 302 radical prostatectomy samples from 114 patients with prostate cancer and was also accessed from the APCB (Supplementary Table 2, Appendix A). Approval was obtained from the Human Research Ethics Committee of the University of South Australia (Application IDs: 201907 and 36070) and Central Adelaide Local Health Network (Application ID: R20181113).

Biomarker identification

Noted pathogenic pathway alterations within the endosome-lysosome system were collated from previous interrogations of online gene expression databases (Omnibus, NCBI, https://www.ncbi.nlm.nih.gov/geo/; Human Protein Atlas, https://www.proteinatlas.org/) and the literature.[17–19] H&E staining and IHC labelling with specific monoclonal antibodies against candidate markers was performed on patient tissue from the pilot cohort. Benign and malignant gland morphologies were initially assessed on H&E stained sections and then re-assessed by IHC. Appl1, Sortilin and Syndecan-1 were selected for further analysis.

Histopathology and immunohistochemistry

Tissue sections (2 μm) were cut from formalin-fixed paraffin-embedded blocks that were representative of the tumour. Sections were stained with routine haematoxylin (Ehrlich's) and eosin (H&E) or labelled by IHC, as previously described.[25] Briefly, heat-induced antigen retrieval was performed in Tris-EDTA Buffer (10 mM Tris Base, 1 mM EDTA Solution, 0.05% Tween-20, pH 9.0). Antibody incubations were carried out at room temperature for 1 h. Detection and visualisation were performed using the EnVision Detection and diaminobenzidine (DAB) chromogenic substrate system (K5007; Dako, USA). The tissue sections were counterstained with Ehrlich's haematoxylin and mounted with DPX mounting media (Merck Millipore,

Australia). All slides were imaged in brightfield with an Axio Scan Z.1 slide scanner (Zeiss, Germany) with a plan-achromat 20× objective.

Development and characterisation of Appl1, Sortilin and Syndecan-1 monoclonal antibodies

Appl1, Sortilin and Syndecan-1 peptides were selected with the aid of AbDesigner using linear sequence analysis, and these were confirmed to represent specific epitopes on the protein surface using modelling of full length sequence predicted with Phyre2.[26,27] To minimise antibody cross-reactivity, unique linear sequence peptides were selected for antibody production, which had no sequence identity with other proteins at the six amino acid level (Supplementary Table 3, Appendix A). The production of all monoclonal antibodies was outsourced to GenScript (USA) for GLP standard production and they were developed in C57BL/6 mice. The specific epitope reactivity was confirmed by western blotting on cell lysate derived from *in vitro* cell lines, and specific cellular localisation confirmed using immuno-fluorescence on cultured cells.[25]

Preparation of cell extracts for western blotting

Cell extracts and western blotting was performed as previously described.[25] Cell line 22Rv1 was obtained from CellBank Australia and cultured in RPMI-1640 media (Gibco, ThermoFisher Scientific, USA). Cells were harvested and extracts prepared using 20 mM Tris (pH 7.0) containing 500 mM sodium chloride and 2% (w/v) SDS and protease inhibitors (Sigma Aldrich, USA), followed by needle shearing and sonication. Total protein was quantified by using a bicinchoninic acid assay method (Micro BCA kit; Pierce, ThermoFisher Scientific). Samples were quantified using a Wallac Victor optical plate-reader and Workout software v2.0 (PerkinElmer, Australia).

For western blotting, briefly, 10 μg of total cell protein from whole cell lysates were heat-denatured, electrophoresed using pre-cast gels (Life Technologies, Australia) and transferred to polyvinylidene difluoride membranes (0.2 μm Polyscreen, PerkinElmer). Membranes were blocked for 1 h at room temperature using 5% (w/v) skim milk or 5% (w/v) BSA in TBS, and subsequently incubated with primary antibody overnight at 4°C with gentle agitation. Membranes were washed in 0.1% (v/v) TBS-Tween-20 and incubated with anti-mouse HRP-conjugated secondary antibody diluted 1:10 000 in 5% milk block. Membranes were visualised using Novex ECL chemiluminescent substrate reagent kit (Life Technologies) and ImageQuant LAS 4000 imager, software version 1.2.0.101 (GE Healthcare, Australia).

Immunofluorescence

PNT2 cells were obtained from CellBank Australia and cultured in RPMI-1640 media (Gibco). DU-145 cells were obtained from American Type Culture Collection (ATCC) and cultured in MEM media (Gibco). Cells were cultured on 13 mm #1.5 coverslips in 24 well plates and formalin-fixed for 10 min, washed three times in PBS and permeabilised with 5% (w/v) BSA in PBS containing 0.05% Saponin. Cells were incubated with primary antibodies overnight at 4°C. Anti-mouse Alexa Fluor 488 (1:1000; Life Technologies) secondary antibody was incubated for 1 h at room temperature. Cells were mounted with ProLong Diamond Antifade Reagent containing DAPI nuclear stain (Life Technologies). Confocal microscopy was performed using a Nikon A1+ laser scanning microscope and associated software (NIS-Elements 4.2; Nikon, Japan). Images were obtained at a resolution of 0.14 μm/px using a 60× objective lens. Exported greyscale 16-bit TIFF files were used to create representative figures in Adobe Photoshop CC (2016; Adobe Systems, USA).

Tissue microarray test cohort

Appl1, Sortilin and Syndecan-1 IHC labelling, and H&E staining was performed on sections from a TMA cohort (*n*=102) consisting of multiple cores per patient (≤5 cores). Morphology was assessed by H&E and protein expression was assessed in analysable samples which consisted of a complete set of Appl1, Sortilin and Syndecan-1 IHC labelling. Non-analysable samples, or samples that did not contain a full set of biomarker labelling (either due to tissue loss or damage from processing or IHC labelling protocol) were excluded from further analysis. The IHC labelling intensity was assessed by H-score with unequivocally labelled (H-score intensity of ≥2), and equivocally labelled (H-score intensity of ≤1).[28]

Radical prostatectomy expansion cohort

As Gleason scoring of the whole tumour cannot be reliably undertaken with TMA samples, the purpose of the radical prostatectomy expansion cohort was to compare the impact of IHC-assisted interpretation of Gleason grading using a multifactorial approach with the biomarkers (described below), versus standard H&E Gleason grade assignment (in terms of both reliability and agreement). Analysable samples (*n*=302) of H&E stained sections and biomarker labelled sections were assigned a Gleason grade and independently reviewed by four specialist uropathologists.

Multifactorial appreciation of Appl1, Sortilin and Syndecan-1 labelling to Gleason grade

Gleason grade by H&E was performed according to standards outlined in the Royal College of Pathologists of Australasia (RCPA) prostate cancer (radical prostatectomy) structured reporting protocol.[29,30] Gleason grade was also assigned from IHC labelled sections using a 'multifactorial appreciation' of the biomarkers, describing the utility of Appl1, Sortilin, and Syndecan-1 labelling as a panel to assess samples, rather than independently utilised markers.

An IHC-assisted Gleason grade using a multifactorial appreciation of Appl1, Sortilin and Syndecan-1 enabled users to determine predominant primary and secondary Gleason patterns in the tissue sections that had a representative tumour. A Gleason grade was only assigned in analysable samples, where a full set of Appl1, Sortilin and Syndecan-1 labelled sections were available.

Statistical analysis

An intraclass correlation test (two-way random effects model) was used to measure the absolute agreement coefficient between users, H&E versus multifactorial IHC-assisted Gleason grade (Appl1, Sortilin and Syndecan as a panel) from the radical prostatectomy expansion cohort. The analysis was undertaken using R version 4.1.1 (https://www.r-project.org/). A senior pathologist then reviewed and verified the Gleason grades based on H&E and IHC slides to produce a consensus Gleason grade.

RESULTS

Biomarker shortlisting and pilot study

Noted gene expression alterations from previously published work identified altered expression of Rab5A (early endosome biogenesis), Appl1 (DCC-interacting protein 13-alpha, subset of early endosomes), EEA1 (early endosome antigen 1, endosome fusion), Rab7A (late endosome marker on compartments with NOX2), NOX2 (NADPH oxidase 2, ROS production in endosomes), ALIX (ALG-2-interacting protein X, multivesicular body biogenesis), Myosin 1B (vesicular traffic), Sortilin (GLUT vesicle biogenesis and regulation), Syntenin (Syndecan-1 binding protein) and Syndecan-1 (cell migration and growth factor uptake) in prostate cancer cells.[17–19] These proteins map to the endosome-lysosome system (Fig. 1) suggesting that this system is a pathogenic pathway for prostate cancer development.

Within the pilot cohort, Appl1, Sortilin and Syndecan-1 monoclonal antibodies demonstrated differential labelling in benign versus well formed and versus poorly formed malignant gland morphologies (Supplementary Fig. 1, Appendix A). Appl1 labelled basal epithelial cells with high intensity and low intensity labelling was observed in adjacent secretory epithelial cells. Well formed malignant glands exhibited moderate labelling with Appl1, while intense labelling was observed in poorly formed malignant glands. Sortilin labelling was absent in benign glands, and well formed malignant glands exhibited a supranuclear polar pattern. In poorly formed malignant glands, labelling was dispersed, lacking intensity and cellular polarity. Syndecan-1 distinguished benign glands by labelling basal cells, similar
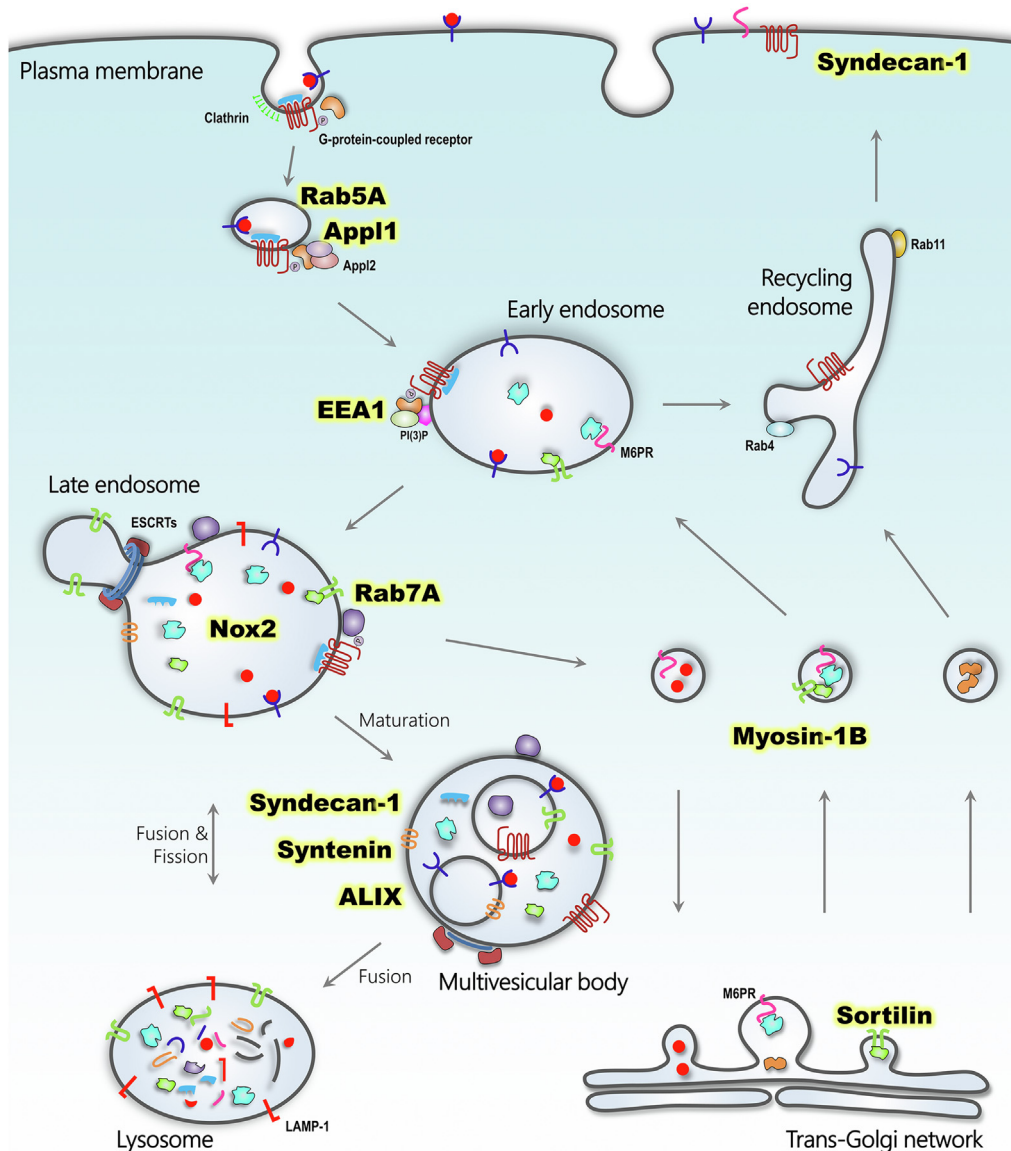
Figure 1   Gene and protein alterations in an endosome-lysosome pathway detected in prostate cancer. Depiction of a potential pathogenic pathway for prostate cancer with endosome-lysosome proteins that represent critical regulatory points (highlighted in yellow).

to Appl1. Well formed malignant glands exhibited minimal labelling, while intense labelling was observed in poorly formed malignant glands (Supplementary Fig. 1, Appendix A). Conversely, IHC labelling for Rab5A, EEA1, NOX2, ALIX, Myosin 1B, Rab7A and Syntenin demonstrated no consistent pattern differences between benign, well formed, or poorly formed malignant glands (Supplementary Fig. 1, Appendix A).

Characterisation of Appl1, Sortilin, and Syndecan-1 monoclonal antibodies

To confirm the specificity of Appl1, Sortilin and Syndecan-1 monoclonal antibodies, specific linear sequences were mapped on the 3D protein structures demonstrating epitope location (Fig. 2A; Supplementary Table 3, Appendix A). Western blot analysis on 22Rv1 cell extracts demonstrated specific single bands with Appl1 (85 kDa) and Sortilin monoclonal antibodies (75 kDa), with the expected molecular weights. Syndecan monoclonal antibody demonstrated two

bands (32 kDa, and 72 kDa), which is the expected molecular weight of monomeric and dimerised Syndecan-1 (32 kDa and 77 kDa, respectively).[31–35] Appl1 and Sortilin immunofluorescence was performed on PNT2 cells, while Syndecan-1 was performed on DU145 cells.

Tissue microarray test cohort

The ability of Appl1, Sortilin and Syndecan-1 antibodies to illustrate various pathologies in the prostate gland was assessed in 102 analysable patient tissues (from 112 patients). H&E was used to identify 66 regions of benign glands, 64 regions of well formed malignant glands and 51 regions of poorly formed malignant glands, which were then assessed by IHC (Supplementary Table 4, Appendix A).

The 100% unequivocal labelling of both Appl1 and Syndecan-1 distinguished benign from malignant glands (i.e., the 66 regions of benign glands identified on H&E were intensely labelled in both the Appl1 and Syndecan-1 IHC sections). Appl1 had unequivocal labelling for 98.4% (63/64)
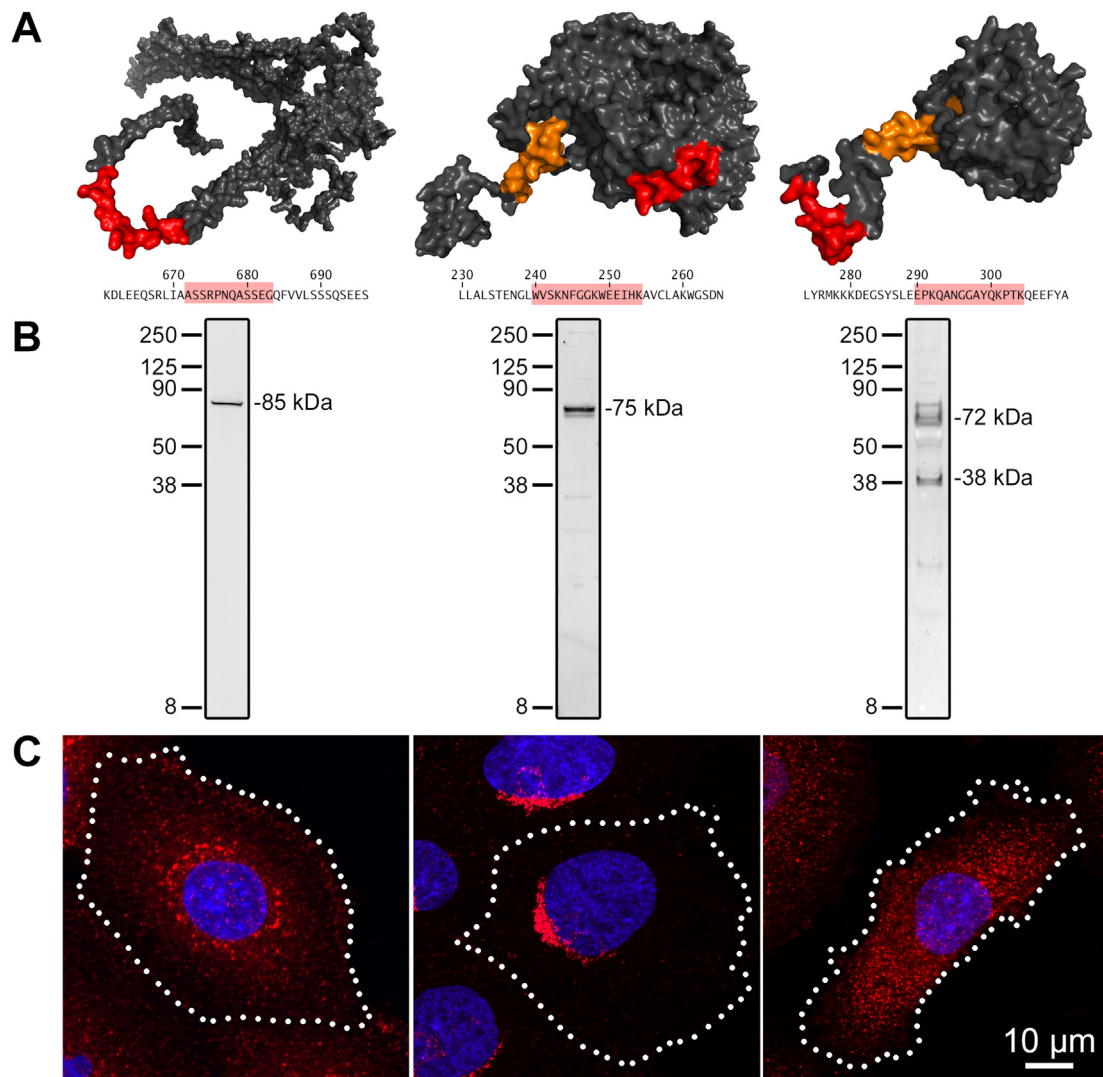
Figure 2 Epitope location and immunochemistry of Appl1, Sortilin and Syndecan-1 specific linear sequence monoclonal antibodies. Unique linear sequences were identified in Appl1 (left), Sortilin (middle) and Syndecan-1 (right) for high specificity monoclonal antibody development. (A) Epitope locations are highlighted in red on the 3D protein structures with the transmembrane regions of Sortilin and Syndecan-1 in orange. (B) Western blotting to detect Appl1 (85 kDa), Sortilin (75 kDa) and Syndecan-1 (major molecular forms at 72 kDa and 38 kDa) was performed using 22RV1 cell extracts. (C) Immunofluorescence with the three monoclonal antibodies detected punctate labelling consistent with the cellular distribution of Appl1 (PNT2 cells), Sortilin (PNT2 cells) and Syndecan-1 (DU145 cells).

of well differentiated regions and 98% (50/51) of poorly differentiated regions within a tumour. Sortilin had un-equivocal labelling for 100% (64/64) of well differentiated regions and 94.1% (48/51) of poorly differentiated regions within a tumour. Syndecan-1 had unequivocal labelling for 100% (66/66) of benign regions, 81.3% (52/64) of well differentiated regions and 92.2% (47/51) of poorly differen-tiated regions within a tumour.

Radical prostatectomy expansion cohort

As Appl1, Sortilin and Syndecan-1 labelled key morphol-ogies within the TMA test cohort, these labelling patterns were evaluated in the expansion cohort (*n*=302 patient sam-ples). Figure 3 demonstrates the ability of Appl1, Sortilin and Syndecan-1 to label benign glands [including low-grade prostatic intraepithelial neoplasia (PIN) versus high-grade PIN], well formed malignant glands, and architectural pat-terns of higher grade cancer, including intraductal carcinoma of prostate (IDCP).

Specifically, in benign prostatic glands, Appl1 and Syndecan-1 labelling clearly detected basal epithelial cells and in each case the biomarkers distinguished luminal epithelial cells (Fig. 3, row 1). Appl1 identified both PIN tissue morphologies, where minimal Sortilin and Syndecan-1 labelling was present (Fig. 3, rows 2 and 3). In well formed malignant glands both Appl1 and Sortilin had increased labelling intensity (compared to benign glands) while Syndecan-1 labelling was minimal (Fig. 3, row 4). In advanced forms of prostate cancer, Appl1 and Syndecan-1 had increased labelling intensity while Sortilin labelling was progressively reduced in poorly formed glands, sheets/ nests of cells, carcinoma with comedonecrosis or IDCP (Fig. 3, rows 5–10). As Appl1, Sortilin and Syndecan-1 labelled key morphologies in prostate cancer biology, the utility of the biomarkers as an IHC panel (a multifactorial appreciation) for Gleason grading was explored.

The biomarker panel was used to interpret both classical and complex morphologies. Punctate and supranuclear fea-tures observed with Sortilin, combined with Syndecan-1
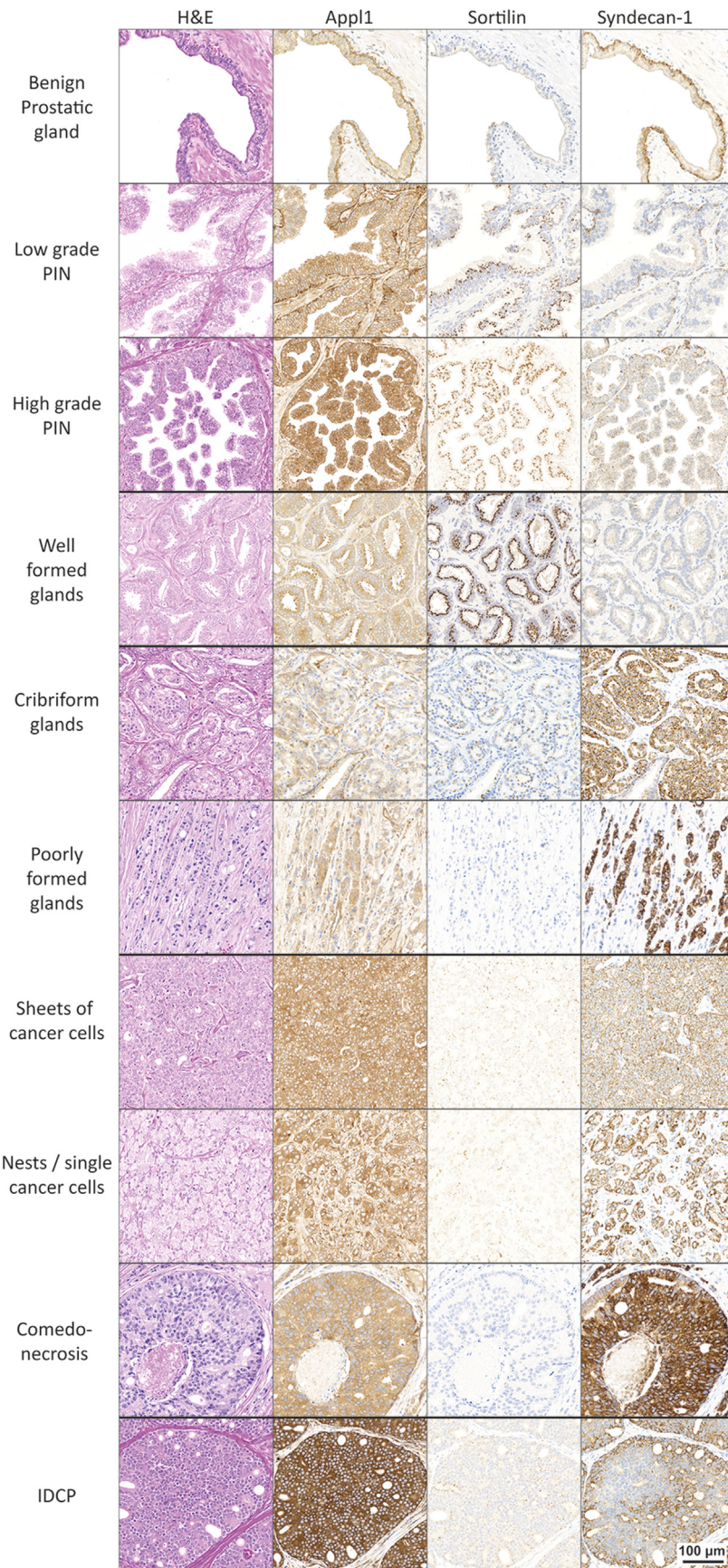
Figure 3 Prostate cancer morphologies visualised by H&E staining or biomarker labelling. Serial sections of tissue from patients with prostate cancer were stained with routine H&E (first column), or labelled with Appl1 (second column), Sortilin (third column) or Syndecan-1 (fourth column). Immunolabelling with Appl1, Sortilin and Syndecan-1 is depicted by a brown immunoprecipitate (DAB). The morphologies identified in routine prostate cancer assessment by H&E included: regions of benign prostatic glands, low grade PIN and high grade PIN; well formed malignant glands; poorly formed malignant and cribriform glands; sheets, nests, single cancer cells and comedonecrosis; and intraductal carcinoma of the prostate (IDCP).

Table 1   Intraclass correlation coefficient; H&E and IHC-assisted Gleason grading according to the current prostate pathology guidelines

	Intraclass correlation (95% CI)	F Test with true value 0			
		Value	df1	df2	Sig
H&E Gleason grade	0.725 (0.684–0.764)	11.5	301	905	0.000
IHC-assisted Gleason grade	0.838 (0.811–0.863)	22.1	301	834	0.000

Single measures, two-way mixed effects model where people effects are random and measures effects are fixed.
df, degrees of freedom.

IHC-assisted Gleason score

H&E Gleason score	Benign	3+3	3+4	4+3	4+4, 5+3	4+5, 5+4	Total
Benign	39	10					49
3+3	12	18	9	1			40
3+4	1	14	49	13	2		79
4+3	1	2	14	23	11	1	52
4+4, 5+3			4	5	18	7	34
4+5, 5+5				2	15	31	48
Total	53	44	76	44	46	39	302

Figure 4   The distribution and agreement of H&E and IHC-assisted Gleason grading according to the current prostate grading guidelines. H&E and IHC-assisted Gleason scoring was in agreement for 59% of the samples (*n*=302). Redistribution of scores determined by IHC markers showed decreased grading for 23% of samples and increased grading for 18% of samples.

labelling below a baseline threshold (basal cell staining intensity in adjacent benign glands), indicated Gleason pattern 3 or well formed malignant glands. When Sortilin labelling featured a loss of granularity and was no longer in a supra-nuclear location, and Syndecan-1 labelling was equal to or above the baseline threshold, this indicated Gleason pattern 4. When Sortilin labelling intensity was minimal or absent, combined with strong Appl1 and Syndecan-1, this indicated Gleason pattern 5 (and was usually associated with cords, sheets and nests of cancer cells). In areas consisting of equivocal Sortilin and Syndecan-1 labelling, Syndecan-1 labelling was referred to as its expression was directly proportional to Gleason pattern and advanced disease. In cases where no benign prostatic glands were available for comparison, Syndecan-1 expression was compared to labelling in plasma cells (specific marker), the endothelial layer of blood vessels, or ganglion nerve cell bodies.

A multifactorial appreciation of Appl1, Sortilin, and Syndecan-1 labelling was investigated by comparing the results with standard H&E assessment. An improved intra-class correlation coefficient (95% CI) was observed using a multifactorial appreciation of Appl1, Sortilin and Syndecan-1 when scoring [0.84 (0.81–0.86)], in comparison to routine H&E [0.73 (0.68–0.76)] (Table 1). This cohort was also independently reviewed to formulate an agreement table comparing IHC-assisted Gleason grade to H&E Gleason grade. Overall, 59% of patient samples in the cohort had agreement (Fig. 4). In the remaining 41%, some samples had a higher IHC-assisted Gleason grade (18% of total number of patient samples), while others had a lower IHC-assisted Gleason grade (23% of total number of patient samples) (Fig. 4). These findings prompted a detailed review of the morphologies contributing to changes in Gleason grade.

In patient samples where H&E and IHC-assisted Gleason grade showed direct alignment, the interpretation of the morphology was clear (Fig. 5). A subset of patient samples with Gleason grade disagreements between H&E and IHC was also examined in three examples (Fig. 6). Each
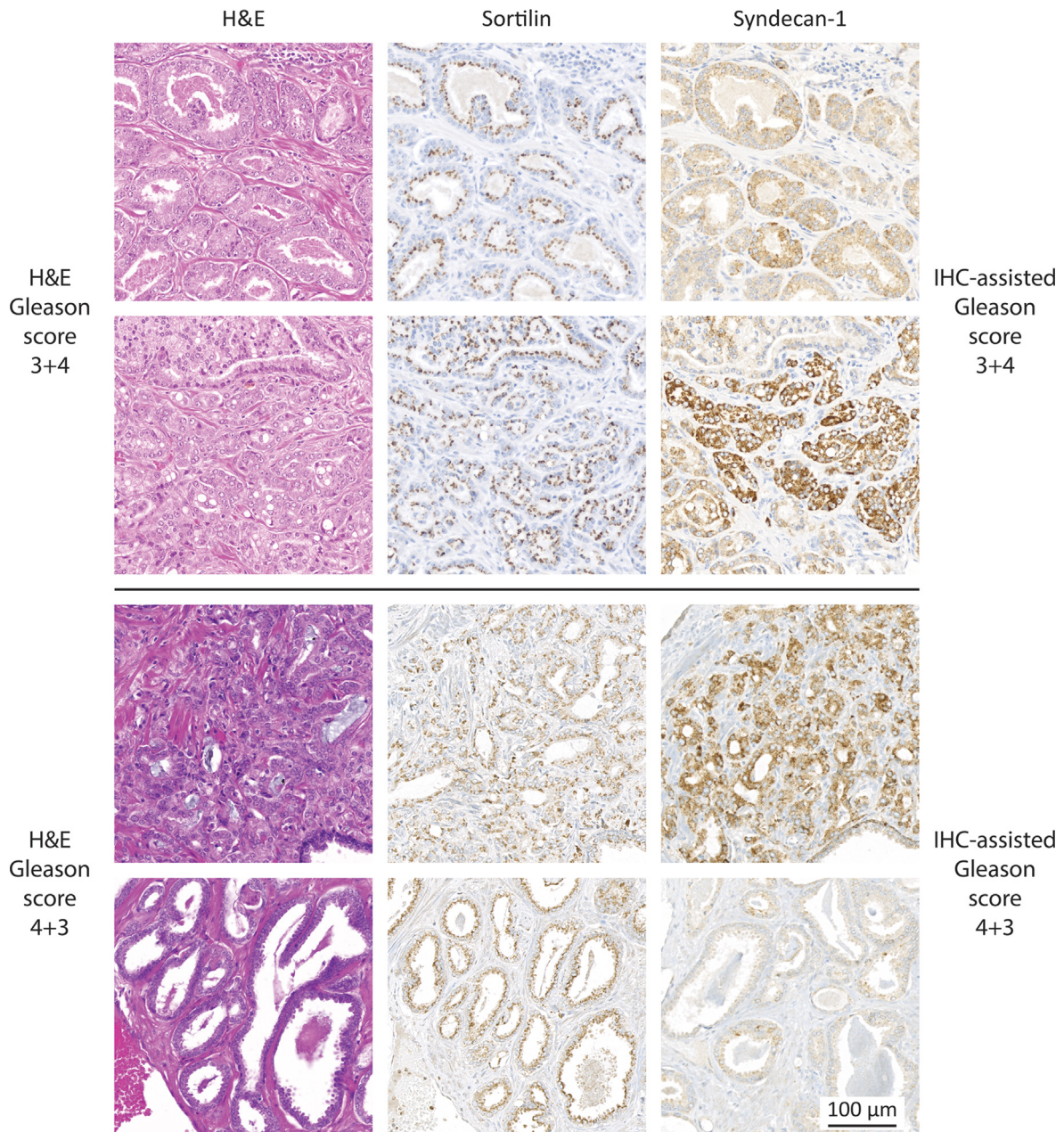
Figure 5   Gleason grade agreement by H&E staining and IHC-assisted biomarker labelling. Gleason grade in patient tissues was assessed using H&E (first column); or IHC-assisted biomarker labelling with Sortilin (second column), and Syndecan-1 (third column) depicted by a brown immunoprecipitate (DAB). Examples of tissue samples from two patients (separated by the black line) with an agreed H&E and IHC-assisted Gleason grade, including Gleason grade 3+4 (rows one and two) and Gleason grade 4+3 (rows three and four). The upper and lower row for each patient represents examples of the different morphologies contributing to the grading. Sortilin immunolabelling indicates the presence of well-formed malignant glands and is confirmed by minimal labelling with Syndecan-1 (top and bottom rows). Syndecan-1 immunolabelling indicates the presence of poorly formed malignant glands and is confirmed by minimal labelling with Sortilin (two middle rows).

example displays primary (top) and secondary (bottom) Gleason patterns. In the top example, assessment by H&E indicated Gleason pattern 4 for both primary and secondary components. IHC-assisted assessment demonstrated a primary component of malignant glands with polar Sortilin labelling (top row; arrowhead), and reduced Syndecan-1 labelling indicated well formed gland morphology (Gleason pattern 3) which reduced the Gleason score from 4+4 with H&E, to 3+4 with IHC (Fig. 6, top two rows). In the middle example, a Gleason score from 3+3 was determined by H&E, but a secondary component of glands (bottom row) displayed loss of granularity of Sortilin which was no longer in a supranuclear location (arrowhead), and high

Syndecan-1 labelling which increased the Gleason score to 3+4 with IHC-assisted assessment (Fig. 6, middle two rows). In the third example (Fig. 6, bottom two rows), a Gleason score of 4+3 was assigned with H&E (reflecting components of cribriform morphology and well formed malignant glands), but IHC assessment with Syndecan-1 visualised cancer cell nests (inset) in addition to the cribriform morphology (top row), which affected the primary and secondary grades. The Gleason score increased from 4+3 with H&E, to 4+5 with IHC-assisted assessment. In the three examples, the multifactorial interpretation of the IHC-assisted biomarker labelling was reconciled upon re-review of the H&E stain.
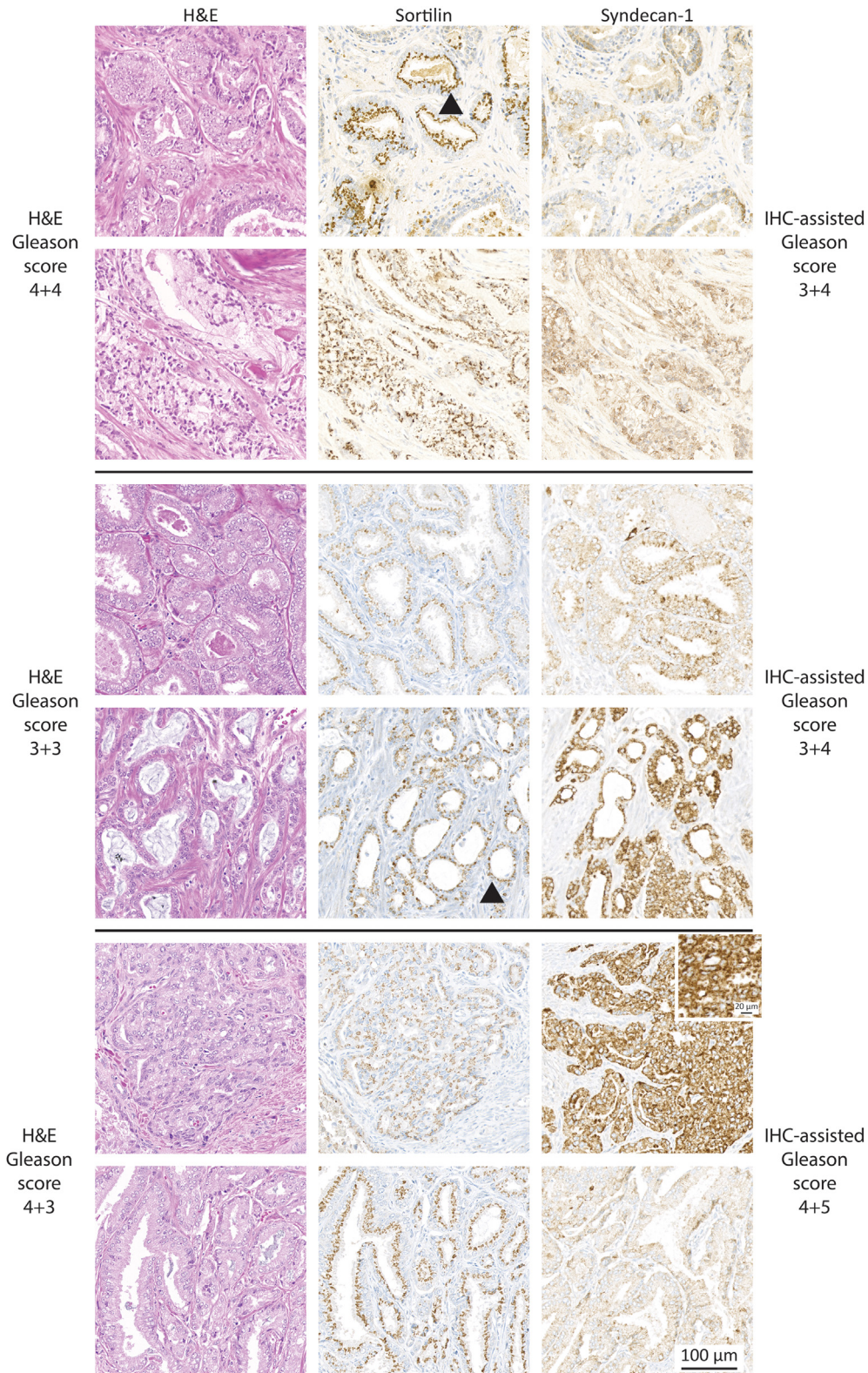
Figure 6 Gleason grade disagreement by H&E staining and IHC-assisted biomarker labelling. Gleason grade in patient tissue assessed using H&E (first column); or IHC-assisted biomarker labelling with Sortilin (second column), and Syndecan-1 (third column) depicted by a brown immunoprecipitate (DAB). Examples of tissue samples from three patients (separated by black lines) with disagreeing H&E and IHC-assisted Gleason grade were assessed (including one downgraded and two upgraded). The upper and lower row for each patient represents examples of the different morphologies contributing to the Gleason grade. In the patient that displayed a reduced Gleason grade compared to H&E (top), Sortilin demonstrated polarised distribution (arrowhead) which indicated the presence of well formed glands, whereas interpretation by H&E suggested only poorly formed gland morphology. Syndecan-1 immunolabelling visualised additional morphology compared to H&E for both patients that were changed to a higher Gleason grade (middle and bottom). The middle example demonstrated high Syndecan-1 expression, combined with Sortilin labelling which was no longer in a supranuclear location (arrowhead; middle). In the bottom example, Syndecan-1 expression identified a component of Gleason pattern 5 (sheets of cancer cells; magnified inset).

DISCUSSION

Prostate cancer pathology assessment is currently reliant on morphological characteristics but does not consider the underlying biology of prostate cancer. Currently, there are no biomarkers that address fundamental problems associated with variable reporting and controversies over the interpretation of morphology and Gleason grade.[7,8,10] For example, AMACR has a role in β-oxidation and cancer metabolic reprogramming, which results in differential expression and variable detection in prostate cancer tissue.[13,36] The endosome-lysosome system has a functional role in all hallmarks of cancer, and therefore has the potential to accurately report on prostate cancer biology.[17–19]

This novel study demonstrated that Appl1, Sortilin and Syndecan-1 monoclonal antibodies developed against unique epitopes reliably inform on the prostate cancer biology by improving morphological interpretation and assist pathology assessment when used as an IHC panel of three biomarkers. These biomarkers were selected from the pilot study based on their capacity to accurately define prostate cancer architecture and to delineate cancer with well formed and poorly formed glands. Using IHC-assisted Gleason grading, the biomarkers increased the reliability of pathology assessment compared with H&E. This study presents the first reliable set of prostate cancer biomarkers, which have the potential to transform clinical pathology practice by standardising the interpretation of the tissue morphology.

Appl1, Sortilin and Syndecan-1 have important functions in the endosome-lysosome system, thus correlate with critical points of pathogenesis in prostate cancer. Characterisation studies demonstrated that the three monoclonal antibodies produced a vesicular and punctate labelling pattern which is consistent with their interaction with intracellular endosomal compartments. Appl1 and Syndecan-1 displayed labelling dispersed through the cytoplasm, while Sortilin demonstrated polarised labelling at supranuclear location which is consistent with localisation to the trans-Golgi network.[37]

Appl1 is a multifunctional endocytic adaptor protein that localises to a specific subset of early endosomes. Appl1 also regulates vesicle transport by controlling the speed of cargo internalisation, while driving endosome signalling in prostate cancer cells.[38,39] Additionally, Appl1 has a role in transcription factor regulation, specifically involving the Wnt signalling pathway.[40] This pathway has a critical role in prostate cancer pathogenesis and has been linked to disease progression and metastatic prostate cancer.[41] The ability to control endosome vesicular traffic and signalling by Appl1 suggests a critical role in the establishment and progression of prostate cancer.

Sortilin belongs to the Vps10p sorting receptor family of proteins and controls the transport of specific intracellular cargo from the trans-Golgi network to endosomes, lysosomes, secretory granules and the plasma membrane.[42] Sortilin is integrally involved in sugar metabolism, being highly expressed in metabolically active tissues and cells. Sortilin acts mechanistically as a transmembrane scaffolding protein to initiate insulin responsive vesicle biogenesis and to bind glucose transporter 4 (GLUT4), as well as facilitate transport to the plasma membrane in response to insulin.[43,44] This critical function of Sortilin in insulin responsive vesicle biogenesis and its location in the trans-Golgi is consistent with the granular perinuclear distribution pattern in prostate cancer tissue. The capacity to interact with both GLUT1 and GLUT4 suggests that Sortilin has a complex role in sugar metabolism, and the increased expression of this biomarker in prostate cancer with well formed glands may indicate a dependence on sugar metabolism for cancer with this morphology.

Syndecan-1 is a transmembrane (type I) heparan sulfate proteoglycan and plasma cell biomarker, also known as CD138, which participates in cell proliferation, migration and cell-matrix interactions.[45,46] In prostate cancer, Syndecan-1 expression was detected in advanced cancer morphologies, including poorly formed glands, nests and cords of cells, cribriform and IDCP. Syndecan-1 has a direct role in growth factor binding and cell migration, and its expression has been associated with biochemical recurrence after radical prostatectomy.[47] This Syndecan-1 biology accounts for its detection in advanced cancer morphologies, as observed in tissue samples from patients with high Gleason grades. Variable Syndecan-1 labelling has previously been reported on prostate tissue.[48] However in this study, a specific Syndecan-1 epitope provided reliable IHC labelling of prostate cancer with poorly formed gland morphology. This indicated that this epitope might have functional significance and have utility for IHC-assisted assessment of advanced prostate cancer.

Gleason grade assessment of prostate carcinoma using H&E staining relies on the subjective interpretation of morphological characteristics, with problems reported for distinguishing benign mimics from cancer, and differentiating well formed from poorly formed cancer glands, reflected as different clonal populations.[9,11,12] The interpretation of transitions between these morphologies can be confounding and therefore it is not surprising that the Gleason grading system has been continually modified to address these problems.[1,5,6,49] In cancer biology, there are classic transitions from benign to dysplasia and neoplasia, as cells lose differentiation, and specifically in prostate cancer these changes align with the morphological transitions originally described by Gleason.[1] A combined appreciation of the three identified biomarkers provides a clear distinction between benign, PIN and neoplastic tissue morphologies, defining the critical cellular transitions with different patterns of biomarker expression. While the expression of Appl1 and Syndecan-1 together provides a clear representation of benign tissue to distinguish it from cancer tissue, further studies are warranted to specifically investigate the biomarker panel's performance against the full breadth of benign mimics of prostate cancer. The utility of the IHC biomarker panel for addressing the striking grade discordance that can often be observed between initial core biopsies and prostatectomy tissue sections is also currently being investigated. A more accurate detection of cancer could reduce patient undertreatment or overtreatment, which respectively results in disease progression or for example, unnecessary surgery and complications. The biomarkers also define the transition between well formed (Gleason pattern 3) and poorly formed cancer gland morphology (Gleason pattern 4). The specific polarised expression pattern for Sortilin defines well formed glands and this aligns with early stage neoplasia, removing any confounding interpretation over this morphology. The critical transition to advanced prostate cancer is characterised by the loss of Sortilin and increased Syndecan-1 expression,

aligning with poorly formed gland morphologies. This highlights the IHC panel as an essential tool for distinguishing between the amount of Gleason patterns 3 and 4, warranting specific biomarker investigation in patient cases where there are questions over Gleason grade 3+4 and 4+3 grading. The combination of Appl1, Sortilin and Syndecan-1 biomarkers provides accurate interpretation of prostate cancer morphology, to improve the reliability of prostate cancer pathology assessment. While further studies may investigate the utility of the IHC biomarker panel assessment, independent of the Gleason system, the combination of both the morphological presentation (Gleason) and the complex biological changes (IHC biomarker panel) may be the most informative and accurate approach for assessing prostate cancer pathology.

Appl1, Sortilin and Syndecan-1, act at critical control points in the endosome-lysosome pathway and, in prostate cancer, these proteins have regulatory roles in transcription factor activity, energy metabolism and cancer progression, accurately informing on the pathogenesis of the disease. This has demonstrated that, by delineating the complex biological changes occurring in prostate cancer, a multifactorial appreciation of these three biomarkers as a panel can improve morphological assessment in patients. This IHC biomarker panel can be used for both training in prostate cancer assessment and as an indispensable tool for accurate grading, which has the potential to transform clinical practice.

APPENDIX A. SUPPLEMENTARY DATA

Supplementary data to this article can be found online at https://doi.org/10.1016/j.pathol.2022.08.001.

Address for correspondence: Dr Carmela Martini, University of South Australia, Bradley Building, City West Campus, North Terrace, Adelaide, SA 5000, Australia. E-mail: carmela.martino@unisa.edu.au

References

1. Gleason DF. Classification of prostatic carcinomas. *Cancer Chemother Rep* 1966; 50: 125–8.
2. Samaratunga H, Delahunt B, Gianduzzo T, *et al*. The prognostic significance of the 2014 International Society of Urological Pathology (ISUP) grading system for prostate cancer. *Pathology* 2015; 47: 515–9.
3. Gleason DF, Mellinger GT. Prediction of prognosis for prostatic adenocarcinoma by combined histological grading and clinical staging. *J Urol* 1974; 111: 58–64.
4. van Leenders GJLH, van der Kwast TH, Grignon DJ, *et al*. The 2019 International Society of Urological Pathology (ISUP) Consensus Conference on Grading of Prostatic Carcinoma. *Am J Surg Pathol* 2020; 44: e87–99.
5. Epstein JI, Allsbrook Jr WC, Amin MB, *et al*. The 2005 International Society of Urological Pathology (ISUP) Consensus Conference on Gleason Grading of Prostatic Carcinoma. *Am J Surg Pathol* 2005; 29: 1228–42.
6. Epstein JI, Egevad L, Amin MB, *et al*. The 2014 International Society of Urological Pathology (ISUP) Consensus Conference on Gleason Grading of Prostatic Carcinoma: definition of grading patterns and proposal for a new grading system. *Am J Surg Pathol* 2016; 40: 244–52.
7. Goodman M, Ward KC, Osunkoya AO, *et al*. Frequency and determinants of disagreement and error in Gleason scores: a population-based study of prostate cancer. *Prostate* 2012; 72: 1389–98.
8. Srigley JR, Delahunt B, Samaratunga H, *et al*. Controversial issues in Gleason and International Society of Urological Pathology (ISUP) prostate cancer grading: proposed recommendations for international implementation. *Pathology* 2019; 51: 463–73.
9. Egevad L, Swanberg D, Delahunt B, *et al*. Identification of areas of grading difficulties in prostate cancer and comparison with artificial intelligence assisted grading. *Virchows Arch* 2020; 477: 777–86.
10. Gansler T, Fedewa SA, Lin CC, *et al*. Trends in diagnosis of Gleason score 2 through 4 prostate cancer in the national cancer database, 1990-2013. *Arch Pathol Lab Med* 2017; 141: 1686–96.

11. Srigley JR. Benign mimickers of prostatic adenocarcinoma. *Mod Pathol* 2004; 17: 328–48.
12. Egevad L, Delahunt B, Furusato B, *et al*. Benign mimics of prostate cancer. *Pathology* 2021; 53: 26–35.
13. Murphy AJ, Hughes CA, Lannigan G, *et al*. Heterogeneous expression of alpha-methylacyl-CoA racemase in prostatic cancer correlates with Gleason score. *Histopathology* 2007; 50: 243–51.
14. Zhou M, Jiang Z, Epstein JI. Expression and diagnostic utility of alpha-methylacyl-CoA-racemase (P504S) in foamy gland and pseudohyper-plastic prostate cancer. *Am J Surg Pathol* 2003; 27: 772–8.
15. Farinola MA, Epstein JI. Utility of immunohistochemistry for alpha-methylacyl-CoA racemase in distinguishing atrophic prostate cancer from benign atrophy. *Hum Pathol* 2004; 35: 1272–8.
16. Gülhan Ö, Mahi B. The role of AMACR, CD10, TMPRSS2-ERG, and p27 protein expression among different Gleason grades of prostatic adenocarcinoma on needle biopsy. *Clin Med Insights Oncol* 2020; 14: 1179554920947322.
17. Johnson IR, Parkinson-Lawrence EJ, Butler LM, *et al*. Prostate cell lines as models for biomarker discovery: performance of current markers and the search for new biomarkers. *Prostate* 2014; 74: 547–60.
18. Johnson IR, Parkinson-Lawrence EJ, Keegan H, *et al*. Endosomal gene expression: a new indicator for prostate cancer patient prognosis? *Oncotarget* 2015; 6: 37919–29.
19. Johnson IR, Parkinson-Lawrence EJ, Shandala T, *et al*. Altered endo-some biogenesis in prostate cancer has biomarker potential. *Mol Cancer Res* 2014; 12: 1851–62.
20. Hanahan D. Hallmarks of cancer: new dimensions. *Cancer Discov* 2022; 12: 31–46.
21. Hanahan D, Weinberg RA. Hallmarks of cancer: the next generation. *Cell* 2011; 144: 646–74.
22. Hanahan D, Weinberg RA. The hallmarks of cancer. *Cell* 2000; 100: 57–70.
23. Yang C, Wang X. Lysosome biogenesis: regulation and functions. *J Cell Biol* 2021; 220: e202192001.
24. Prabhakaran S, Woo WLW, Xing G, *et al*. The incidence of labelling of non-lung adenocarcinomas with antibodies against TTF-1 and diagnostic implications. *Appl Immunohistochem Mol Morphol* 2020; 28: 471–6.
25. Johnson IRD, Sorvina A, Logan JM, *et al*. A paradigm in immuno-chemistry, revealed by monoclonal antibodies to spatially distinct epi-topes on Syntenin-1. *Int J Mol Sci* 2019; 20: 6035.
26. Pisitkun T, Hoffert JD, Saeed F, *et al*. NHLBI-AbDesigner: an online tool for design of peptide-directed antibodies. *Am J Physiol Cell Physiol* 2012; 302: C154–64.
27. Kelley LA, Mezulis S, Yates CM, *et al*. The Phyre2 web portal for protein modeling, prediction and analysis. *Nat Protoc* 2015; 10: 845–58.
28. O'Hurley G, Perry AS, O'Grady A, *et al*. The role of secreted frizzled-related protein 2 expression in prostate cancer. *Histopathology* 2011; 59: 1240–8.
29. The Royal College of Pathologists of Australasia (RCPA). *Prostate Cancer (Radical Prostatectomy) Structured Reporting Protocol: (3rd Edition)*. Sydney: RCPA, 2018. https://www.rcpa.edu.au/Library/Practising-Pathology/Structured-Pathology-Reporting-of-Cancer/Cancer-Protocols/Genitourinary/Protocol-prostate-cancer-radical-prostatectomy.aspx
30. Kench JG, Judge M, Delahunt B, *et al*. Dataset for the reporting of prostate carcinoma in radical prostatectomy specimens: updated rec-ommendations from the International Collaboration on Cancer Report-ing. *Virchows Archiv* 2019; 475: 263–77.
31. Holmes RM, Yi Z, De Filippis E, *et al*. Increased abundance of the adaptor protein containing pleckstrin homology domain,

phosphotyrosine binding domain and leucine zipper motif (APPL1) in patients with obesity and type 2 diabetes: evidence for altered adipo-nectin signalling. *Diabetologia* 2011; 54: 2122–31.
32. Mazella J, Zsurger N, Navarro V, *et al*. The 100-kDa neurotensin re-ceptor is gp95/sortilin, a non-G-protein-coupled receptor. *J Biol Chem* 1998; 273: 26273–6.
33. Massa F, Devader C, Lacas-Gervais S, *et al*. Impairement of HT29 cancer cells cohesion by the soluble form of neurotensin receptor-3. *Genes Cancer* 2014; 5: 240–9.
34. Saunders S, Jalkanen M, O'Farrell S, *et al*. Molecular cloning of syndecan, an integral membrane proteoglycan. *J Cell Biol* 1989; 108: 1547–56.
35. Manon-Jensen T, Multhaupt HA, Couchman JR. Mapping of matrix metalloproteinase cleavage sites on syndecan-1 and syndecan-4 ecto-domains. *FEBS J* 2013; 280: 2320–31.
36. Magi-Galluzzi C, Luo J, Isaacs WB, *et al*. Alpha-methylacyl-CoA racemase: a variably sensitive immunohistochemical marker for the diagnosis of small prostate cancer foci on needle biopsy. *Am J Surg Pathol* 2003; 27: 1128–33.
37. Petersen CM, Nielsen MS, Nykjaer A, *et al*. Molecular identification of a novel candidate sorting receptor purified from human brain by receptor-associated protein affinity chromatography. *J Biol Chem* 1997; 272: 3599–605.
38. Diggins NL, Webb DJ. APPL1 is a multifunctional endosomal signaling adaptor protein. *Biochem Soc Trans* 2017; 45: 771–9.
39. Wu KKL, Long K, Lin H, *et al*. The APPL1-Rab5 axis restricts NLRP3 inflammasome activation through early endosomal-dependent mitoph-agy in macrophages. *Nat Commun* 2021; 12: 6637.
40. Banach-Orlowska M, Szymanska E, Miaczynska M. APPL1 endocytic adaptor as a fine tuner of Dvl2-induced transcription. *FEBS Lett* 2015; 589: 532–9.
41. Sandsmark E, Hansen AF, Selnaes KM, *et al*. A novel non-canonical Wnt signature for prostate cancer aggressiveness. *Oncotarget* 2017; 8: 9572–86.
42. Canuel M, Korkidakis A, Konnyu K, *et al*. Sortilin mediates the lyso-somal targeting of cathepsins D and H. *Biochem Biophys Res Commun* 2008; 373: 292–7.
43. Bogan JS, Kandror KV. Biogenesis and regulation of insulin-responsive vesicles containing GLUT4. *Curr Opin Cell Biol* 2010; 22: 506–12.
44. Pan X, Zaarur N, Singh M, *et al*. Sortilin and retromer mediate retro-grade transport of Glut4 in 3T3-L1 adipocytes. *Mol Biol Cell* 2017; 28: 1667–75.
45. Chilosi M, Adami F, Lestani M, *et al*. CD138/syndecan-1: a useful immunohistochemical marker of normal and neoplastic plasma cells on routine trephine bone marrow biopsies. *Mod Pathol* 1999; 12: 1101–6.
46. Wang S, Zhang X, Wang G, *et al*. Syndecan-1 suppresses cell growth and migration via blocking JAK1/STAT3 and Ras/Raf/MEK/ERK pathways in human colorectal carcinoma cells. *BMC Cancer* 2019; 19: 1160.
47. Shimada K, Anai S, Fujii T, *et al*. Syndecan-1 (CD138) contributes to prostate cancer progression by stabilizing tumour-initiating cells. *J Pathol* 2013; 231: 495–504.
48. Santos NJ, Barquilha CN, Barbosa IC, *et al*. Syndecan family gene and protein expression and their prognostic values for prostate cancer. *Int J Mol Sci* 2021; 22: 8669.
49. van Leenders G, van der Kwast TH, Iczkowski KA. The 2019 Inter-national Society of Urological Pathology Consensus Conference on Prostate Cancer Grading. *Eur Urol* 2021; 79: 707–9.